GISAXS - Glancing incidence small angle X-ray scattering

J. Levine Parrill, P. Georgopoulos, Y.-W. Chung, J. Cohen

HAL Id: jpa-00252316
https://hal.archives-ouvertes.fr/jpa-00252316

Submitted on 1 Jan 1993

GISAXS - Glancing incidence small angle X-ray scattering

J.R. LEVINE PARRILL, P. GEORGOPOULOS*, Y.-W. CHUNG* and J.B. COHEN*

IBM, East Fishkill, EM1, Route 52, Hopewell Junction, NY 12533, U.S.A.
* Department of Materials Science and Engineering, McCormick School of Engineering and Applied Science, Northwestern University, Evanston, IL 60208, U.S.A.

ABSTRACT

In this method, the incident beam is totally externally reflected from a surface or substrate, followed by small-angle scattering of the refracted (evanescent) beam by the surface region. As one example, GISAXS can provide size information on islands associated with film growth. The technique is described, along with examples from studies of Au on glass, and InAs on silicon. In contrast to TEM this technique is nondestructive, can be done in situ, provides excellent sampling, does not necessarily require synchrotron radiation, and is not limited to thin or conducting substrates.

INTRODUCTION

The basic experimental arrangement, first discussed in 1988 [1], is illustrated in Fig. 1. Because x-rays have an index of refraction slightly less than unity, there is total <u>external</u> reflection, at low angles of incidence (a few mrad). As well as the reflected beam, there is a refracted beam which at the critical angle for reflection, travels along the surface and penetrates only a few tens of Angstroms, Fig. 2: for this reason it is referred to as an evanescent wave. This evanescent wave can act as a source for diffraction from near surface regions, as first demonstrated by Marra, Eisenberger and Cho in 1979 [2], for wide-angle diffraction from planes perpendicular to a film surface.

This surface wave can be a source for small angle scattering and is particularly useful for parameterizing islands in thin film growth. In this paper, after discussing some special features of this method, we give examples of Au islands on glass, and InAs forming on Si. For further details, see references [3-5]. The method was actually discovered about the same time as our group by Naudon and coworkers [6]. Their use was to examine clustering near surfaces, as compared to the bulk.

The Technique
The experimental arrangement, using a position sensitive detector, is illustrated in Fig. 3, where it is seen that the detector is carefully positioned to avoid the reflection and beam spillover.

There are several points in the theory of small angle scattering that need consideration. The usual equation for small angle scattering, Eq. 1, needs modification:
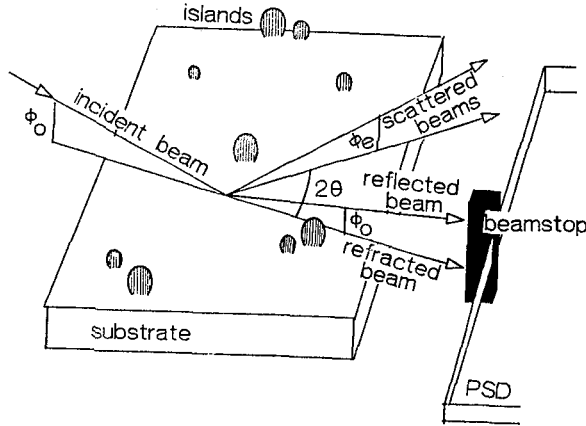
Figure 1. Experimental scattering geometry for GISAXS. The angle 2θ is measured in the plane of the sample surface. The angles ϕ_0 are in a plane perpendicular to the sample surface. The position sensitive detector (PSD) is parallel to the surface. The refracted beam illuminates surface features which produce SAXS at $0° < 2\theta < 4°$.
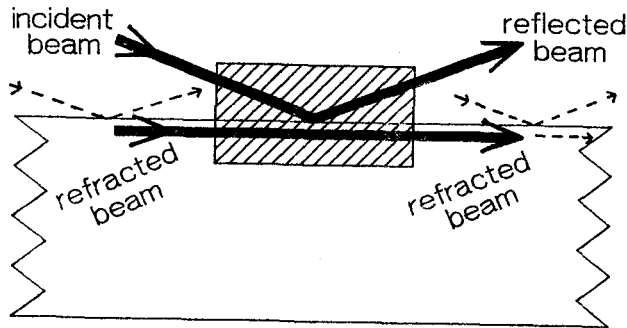

Figure 2. Dotted rays indicate reflection/refraction reactions occur all along infinite surface having islands.

$$I_{SAXS}(h) = I_e(h)(\Delta\rho_e)^2 tA_iN_V e^{-\mu t}\sum_R V_p^2(R)\Phi^2(hR)Z(R) \tag{1}$$

In this equation, t is the sample thickness, A_i the irradiated area, and N_V the number of particles per unit volume and the other terms have their usual meaning. The product tA_iN_V becomes A_iN_a where N_a is the number of scattering regions per unit area. For the absorption $e^{-\mu t}$, t is the refracted beam penetration, L and with ϕ the incident angle:

$$L = \frac{\lambda}{2\pi\left(\phi_c^2 - \phi^2\right)^{1/2}} \tag{2a}$$
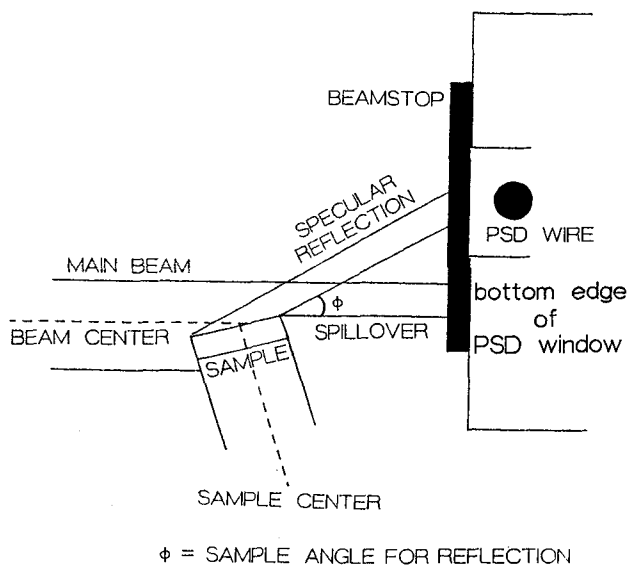
ϕ = SAMPLE ANGLE FOR REFLECTION

Figure 3. Configuration of incident beam spillover, PSD, specular reflection, beamstop, and sample for correct GISAXS alignment.
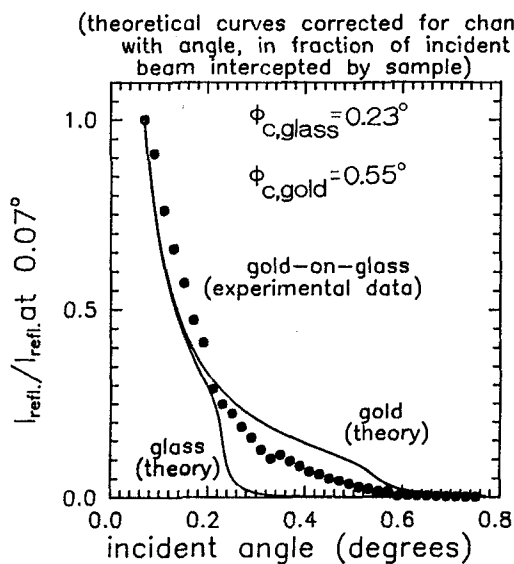

Figure 4. Dots are reflected intensity as a function of incident angle from a gold on glass sample with a 40% gold coverage. Solid curves are the variations with angle of the theoretical reflectivity coefficients.

where the critical angle, ϕ_C is:

$$\phi_c = \lambda \left(\frac{\rho_e r_e}{\pi} \right)^{1/2} \tag{2b}$$

The term I_0 becomes $f\, I_{refr}$: were f is fraction of the refracted beam intercepted, and:

$$I_{refr} = \frac{4\phi^2}{(\phi_c + p)^2 + q^2} \tag{3a}$$

$$p^2 - q^2 = \phi^2 - \phi_c^2 \tag{3b}$$

$$pq = \beta \tag{3c}$$

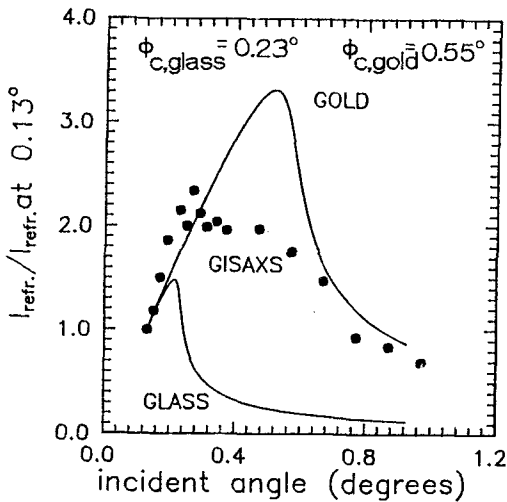$$\beta = \mu\lambda/4\pi \tag{3d}$$

Figure 5. Dots are GISAXS intensity as a function of incident angle at $h \approx 0.05$ Å^{-1} from a gold on glass sample with a 40% gold coverage. Solid curves are the variations with angle of the evanescent wave for gold and glass. Theoretical intensities are corrected for fraction of incident beam intercepted. Optimum GISAXS intensity is obtained near the critical angle for glass.
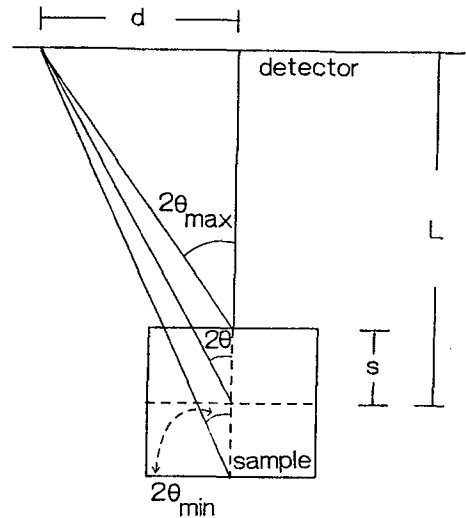

Figure 6. Illustration of effect of range of sample to detector distance on GISAXS.

If we take as an example, Au islands ($\approx$ 24Å in radius) on glass, Fig. 4 illustrates the measured reflectivity (points) and those calculated (solid line), and similarly for the refracted wave, Fig. 5. It is clear that both the islands and the glass contribute, but as the islands are only ~ 24Å thick in this case and there is only 40% coverage, the refracted wave from the Au passes along the glass as well.

Figure 6 illustrates that in a reflection geometry the source of scattering covers dimensions much larger than the usual micron or so sample thickness in transmission

SAXS. With the detector at a distance of several hundred mm, there is no significant distortion of the scattering [5].

Gold on Glass [4,5].

Typical patterns are given in Fig. 7 for average film thicknesses of 5, 9 and 13 Å. At these coverages (up to 40%) there is strong interparticle interference in the scattering, and there is no Guinier region. Nevertheless, the Porod radius (or the surface to volume ratio) can be determined, and from the peak in the scattering, the interparticle distance. Size comparisons with TEM reveal that the particles are hemispherical and from fractal analysis they are smooth.

The patterns are actually two dimensional. Fig. 8 is a digitized film of the pattern, on one side of the direct beam, and above the sample. From the data normal to the film the size in that direction may also be determined and such results indicated that the particles are slightly flattened.
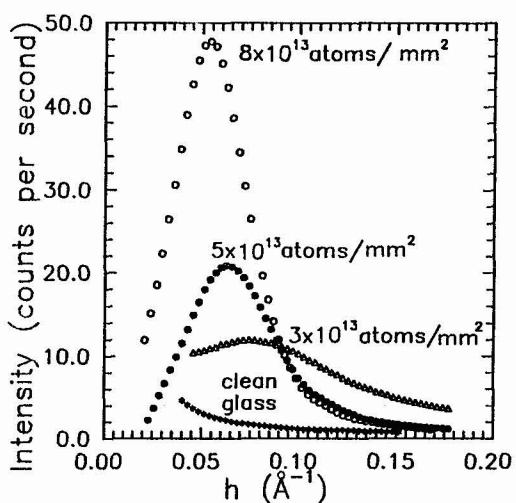

Figure 7. GISAXS data for three gold films with different average thicknesses; scattering from clean glass included for reference.
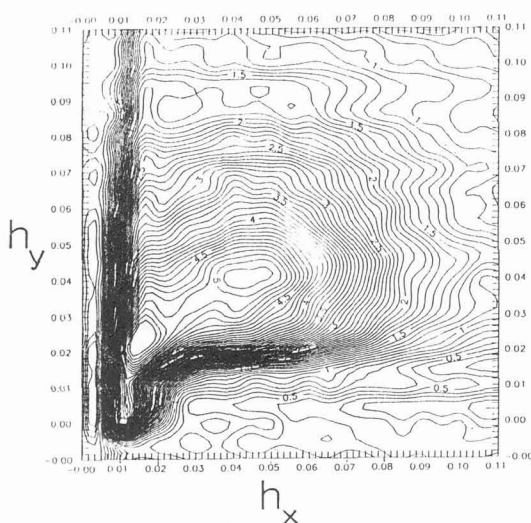
Figure 8. Topographic map of two-dimensional GISAXS pattern from Au islands.

In ref. 4, kinetic data were taken during deposition (in a UHV environment), and in situ, after annealing for various times and temperatures. The particles grew in size and decreased in number by soft impingement, diffusion-limited mobile island growth [4]. The activation energy and diffusion coefficient for the process are of the same magnitude as values for single-atom surface diffusion. Coarsening models (which predict a power law dependence on time, $t^{1/n}$) are not adequate.

InAs on Si (5)

As another example, InAs films were prepared in UHV by C. H. Choi [7], using low energy ion beam bombardment assisted molecular beam epitaxy. Sample 1 contains 30

monolayers of InAs, 2 has 16, and 3, 15. For No. 1 the arsenic cell was at 593°K and the ion beam was 30 eV, for No. 2, 613°K and 15 eV and for No. 3, 613°K and 30 eV. The samples one and three have rounded islands, whereas in 2, there were facets.

The scattering patterns are shown in Fig. 9, and the Porod plots in Fig. 10. (The Guinier regions are behind the beam stop). The sizes are of the order of 50Å.
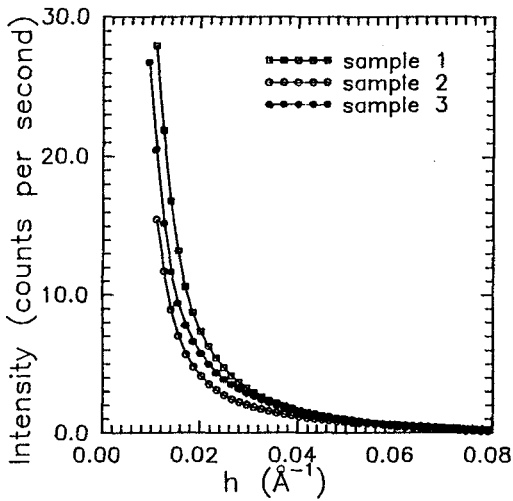

Figure 9. GISAXS data for three InAs films on Si substrates. InAs has layer plus island morphology.
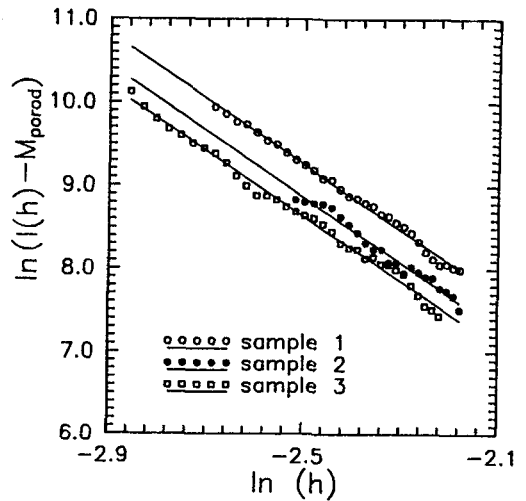
Figure 10. Porod plots for InAs/Si samples. Slopes are approximately -4 and data has been corrected for background contributions by substracting slopes of power Porod plots.

ACKNOWLEDGEMENTS

REFERENCES

[1]   Levine, J.R., Y.W.Chung, Cohen, J.B. and Georgopoulos, P., J. Vac. Sci. Technol., **A6(3)** (1988) 1771.

[2]   Marra, W.C., Eisenberger, P. and Cho, A.Y., J. Appl. Phys., **50** (1979) 6927.

[3]   Levine, J.R., Cohen, J. B., Chung, Y.W. and Georgopoulos, J. Appl. Cryst., **22** (1989) 528.

[4]   Levine, J.R., Cohen, J. B. and Chung, Y.W., Surface Science, **248** (1991) 215.

[5]   Levine, J.R., Ph.D. Thesis, Northwestern University, 1990.

[6]   Naudon, A., Slimani, T. and Goudeau, P., J. Appl. Cryst., **24** (1991) 501.

[7]   Choi, C.H., Huttman, L. and Barnett, S.A., J. Vac. Sci. Technol., **A8** (1990) 1587.